

EUROPEAN ORGANISATION FOR NUCLEAR RESEARCH

European Laboratory For Particle Physics

INTERNAL REPORT

TIS-RP/IR/2000-09

14 April 2000

A New Calibration of the PIC Monitor in H6

Edda Gschwendtner, Angela Mitaroff and Luisa Ulrici

CERN, 1211 Geneva 23, Switzerland

Abstract

In 1999 the beam monitor of CERF (a Precision Ionisation Chamber - PIC) was calibrated by comparing its response with the reading of the Trigger4 beam scintillator installed in the H6 beam line. Two independent measurements with different beam intensities, different data processing and analysis methods were performed. The combination of the two experiments gives at 120 GeV/c beam momentum a calibration factor of $\Gamma_{120}=(23264 \pm 945)$ particles/PIC-count. In addition the calibration factor Γ at $p=40$ GeV/c was measured during the low beam intensity runs. We get a calibration factor of $\Gamma_{40}=(24475 \pm 674)$ particles/PIC-count which is consistent with the fact that the energy loss in the PIC-counter is lower at a beam momentum of 40 GeV/c.

Contents

1	Introduction	3
2	Measurements and Analysis	4
2.1	Experimental Set Up	4
2.2	Background and Low Intensity Measurements	6
2.3	Analysis of the Low Intensity Measurements	8
2.4	High Intensity Measurements	14
2.5	Analysis of the High Intensity Measurements	14
3	Results	18
4	Summary and Conclusion	19

1 Introduction

The intensity of the SPS secondary beam to the CERN-EU High Energy Reference Radiation Facility CERF [Bir97] is monitored by a Precision Ionisation Chamber (PIC). All the data of the experiments performed at CERF are normalised to the intensity of the secondary beam in order to compare them. For this reason an exact knowledge of the calibration factor of the PIC is necessary.

In 1993/94 a series of activation measurements were done, using plastic scintillators, graphite plates and polyethylene foils [Car93, Hoo93, Liu93, Roe94, Ste94a, Ste94b]. These measurements gave a calibration factor of $2.2 \cdot 10^4$ beam particles per PIC-count, with an uncertainty of $\pm 10\%$. This value was used as reference since then.

In 1998 a verification of the PIC calibration was done by comparing the responses of the PIC-counter with three scintillators installed in the H6-beam line [Els98]. The results of these measurements showed that the calibration factor is in agreement with the 1993/94 measurements. This year the calibration factor of the PIC was newly measured in a more precise way, i.e. measuring the background and subtracting it from the detector signals, correcting the scintillator signal according to its dead time and doing a proper error analysis.

The new measurements were performed at CERF on 27 May 1999 with positive hadrons with a momentum of 120 GeV/c and from 5 to 13 August 1999 with a beam of $p=120$ GeV/c and $p=40$ GeV/c positive hadrons.

2 Measurements and Analysis

2.1 Experimental Set Up

Beam

The experiments took place in the CERF test area along the H6-beam line, housed in building EHN1 (SPS north experimental hall). The H6-beam line is a secondary beam, produced by the primary SPS beam hitting a Be-target T4. The total SPS cycle lasted 14.4 s with a spill ('beam on') of 2.58 s during the low intensity measurements and 2.37 s during the high intensity measurements [Ard00]. The H6-beam consists of different percentages of protons, pions and kaons depending on the momentum that can be tuned between $p=10$ GeV/c and $p=205$ GeV/c. The following calibration measurements were performed with $p=40$ GeV/c and $p=120$ GeV/c. In Table 1 the composition of the beam at the position of the PIC-counter is shown [Vin99].

Table 1: H6-beam particle composition for $p=40$ GeV/c and $p=120$ GeV/c .

beam momentum	pions (π^+)	protons	kaons (k^+)
40 GeV/c	85%	12%	3%
120 GeV/c	61%	35%	4%

PIC-counter

The PIC-counter is installed about 405 m downstream of the T4 production target. It is an open air Ionisation Chamber with cylindrical shape. Its sensitive volume is 0.86 litres (diameter: 185 mm, active length: 32 mm). The charge produced by ionisation of the beam in this volume is collected at a capacitor. Whenever this charge reaches a certain value, the capacitor is discharged and we get one count that is proportional to the number of beam particles which have produced this charge.

Beam Scintillator Trigger4

The Trigger4 beam scintillator is installed 40 m upstream of the PIC-counter. It is normally used for aligning the beam. This scintillator has a diameter of 10 cm, is 2 mm thick and half of it is surrounded by a perspex light-guide. The beam scintillator gives a signal for each particle in the beam.

First, a good operating point of this scintillation counter must be chosen. For this, we varied the high voltage of the photo-multiplier (PMT) and recorded the counts of the scintillator normalised to the primary particles hitting T4. As we see from Figure 1 a good operating region lies between $U=-2.05$ kV and $U=-2.15$ kV. For the calibration measurements the high voltage of the scintillator was set to $U=-2.1\pm 0.05$ kV.

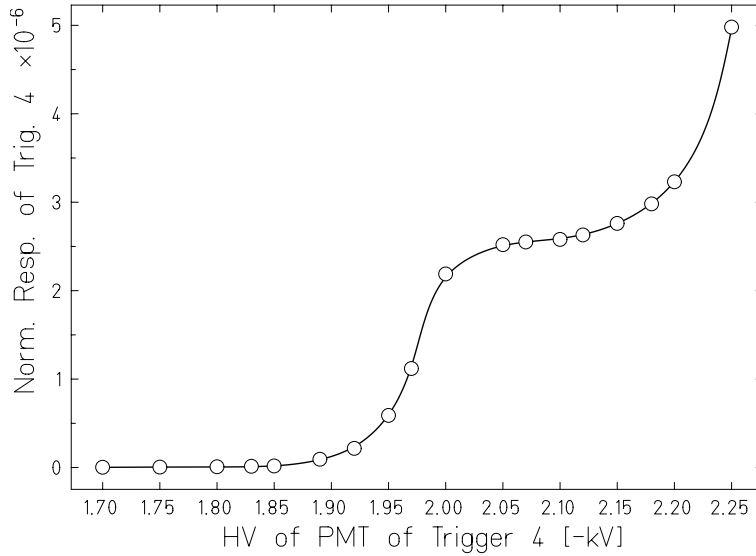


Figure 1: Counts of the beam scintillator Trigger4 normalised to the primary particles on the production target T4 as a function of high voltage (HV) of the photo-multiplier (PMT). A good operating point of the beam scintillator lies between $U=-2.05\text{ kV}$ and $U=-2.15\text{ kV}$.

Overview of the Measurements

In order to calculate the calibration factor Γ of the PIC giving the relation between PIC-counts and the number of particles in the beam we compared the PIC-counts with the beam scintillator counts. For that purpose we varied the beam intensity in the range between 10 to 210 PIC-counts per spill (chapter 2.3) and between 55 to about 8000 PIC-counts per spill (chapter 2.4). Different intensities were achieved by adjusting the aperture of 4 collimators (i.e. C3, C5, C10, C11) along the H6-beam line.

The data for the background and low intensity measurements were acquired during the 'ATLAS Background Benchmarking Measurements' [Gsc00b]. The analog beam scintillator signals were driven to a discriminator with a threshold of 100 mV and an output signal of about 60 ns duration. For each spill the signals of the PIC-counter and the beam scintillator were counted in a CAMAC-scaler and written to tape. Usually for one collimator setting data were taken from about 100 spills. The counting time in each spill was not the total spill length (i.e. 2.58 s) but 2.0 seconds in order to avoid any 'edge effects'.

The high intensity data were acquired during the CERF measurements. The PIC counts were read out online with a LabView Program running on a PC. The beam scintillator counts were provided directly by a SPS-beam-control program. The counting time lasted the entire spill length (i.e. 2.37 s). For each collimator setting data of 3 spills were taken.

2.2 Background and Low Intensity Measurements

Seven different low intensity measurements for the PIC calibration were performed. Three of them with 120 GeV/c beam momentum (runs I, II, III) and four of them with 40 GeV/c beam momentum (IV, V, VI, VII). For each run data of more than 100 spills were taken.

Background Measurements

Even when the H6-beam is switched off Trigger4 and the PIC-counter are counting. This can be due to the fact that other beam lines with a big muon halo are close to the H6-beam line, some particles from the target T4 can still reach the counters or due to remanent radioactivity. So before each of the runs I→VII the

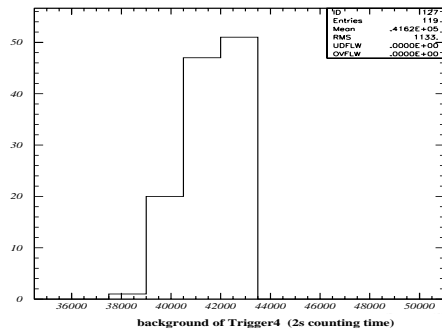


Figure 2: Beam scintillator background for run number Ia. The beam momentum is 120 GeV/c.

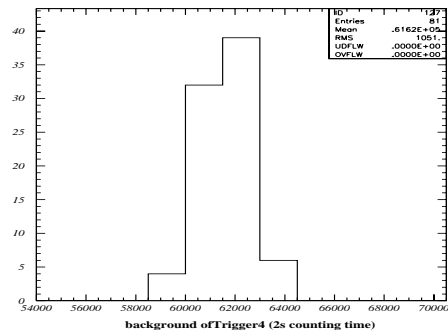


Figure 3: Beam scintillator background for run number VIIa. The beam momentum is 40 GeV/c.

background was measured by switching off the magnets of the H6-beam line and by using the same collimator settings in order to exclude any additional effects on the background (measurements Ia, IIa, IIIa, IVa, Va, VIa, VIIa). As an example, Figure 2 shows the Trigger4 background measurement of run Ia for the corresponding 'beam on' run I. In Figure 3 we see the Trigger4 background of run VIIa.

Table 2: PIC-counter and Trigger4 background during 2s counting time for different beam intensities at 120 GeV/c beam momentum.

run number	C3 [mm]	C5 [mm]	C10 [mm]	C11 [mm]	spills/run	PIC background	Trigger4 background
Ia	±4	±4	±2	±1.5	119	1.20 ± 0.40	41644 ± 1133
IIa	±30	±20	±2	±1.5	183	1.13 ± 0.33	37137 ± 776
IIIa	±20	±20	±2	±2	118	1.33 ± 0.47	41254 ± 1927

Tables 2 and 3 give a summary of the background measurements. For every run they show the apertures of the collimators, the number of spills for which data

Table 3: PIC-counter and Trigger4 background during 2s counting time for different beam intensities at 40 GeV/c beam momentum.

run number	C3 [mm]	C5 [mm]	C10 [mm]	C11 [mm]	spills/run	PIC background	Trigger4 background
IVa	± 5	± 45	± 3	± 3	61	0.70 ± 0.46	64305 ± 1389
Va	± 12	± 45	± 5.5	± 3	100	0.52 ± 0.50	59178 ± 912
VIa	± 35	± 45	± 5.5	± 5.5	134	0.68 ± 0.47	59223 ± 1002
VIIa	± 35	± 45	± 5.5	± 5.5	81	0.58 ± 0.49	61722 ± 1052

were taken, the average PIC background and the average Trigger4 background. According to the width of the discriminator output signal the Trigger4 data are corrected for a dead time of $\tau = 60$ ns. The errors are the standard deviations of the histograms.

Low Intensity Measurements

After each background measurement the calibration measurements were performed. Table 4 shows for each run with a momentum of 120 GeV/c the number of spills, the average PIC values and the average Trigger4 counts that are corrected for dead time. Table 5 shows the measurement results for $p=40$ GeV/c. The corresponding background values for the PIC-counter and Trigger4 are already subtracted.

Table 4: Averaged PIC and Trigger4 counts during 2s counting time for different beam intensities at $p=120$ GeV/c.

run number	spills/run	PIC- bg_{PIC}	Trigger4- $bg_{Trigger4}$
I	183	10.3	$2.4 \cdot 10^5$
II	151	96.4	$22.6 \cdot 10^5$
III	177	117.9	$27.7 \cdot 10^5$

Table 5: Averaged PIC and Trigger4 counts during 2s counting time for different beam intensities at $p=40$ GeV/c.

run number	spills/run	PIC- bg_{PIC}	Trigger4- $bg_{Trigger4}$
IV	211	11.5	$2.9 \cdot 10^5$
V	283	42.0	$10.2 \cdot 10^5$
VI	142	180.0	$43.4 \cdot 10^5$
VII	181	208.2	$50.2 \cdot 10^5$

2.3 Analysis of the Low Intensity Measurements

In order to know the calibration factor γ of a run, we plot for each spill the fraction

$$r = \frac{Trigger4 - \langle bg_{Trigger4} \rangle}{PIC - \langle bg_{PIC} \rangle}. \quad (1)$$

into a histogram. The values are read out for each spill and $Trigger4$ is corrected for dead time with $\tau = 60$ ns. $\langle bg_{Trigger4} \rangle$ and $\langle bg_{PIC} \rangle$ are the corresponding averaged background values from Tables 2 and 3. As an example, we see in Figure 4 the histogram of the ratio r for run III ($p=120$ GeV/c). Figure 5 shows the results for run V ($p=40$ GeV/c). The final PIC calibration factor Γ is then achieved by taking the weighted mean values $\langle r \rangle$ of the different runs (see below).

For a single run the mean value of the ratio $\langle r \rangle$ is the calibration factor γ . However, the statistical error $\Delta\gamma$ is not the width Δr of the histograms, since this includes also the errors of the Trigger4 background $bg_{Trigger4}$ and not only the errors of the PIC-counter such as the ones of bg_{PIC} , binning, etc. We therefore have to subtract the error component $\Delta bg_{Trigger4}$ from Δr .

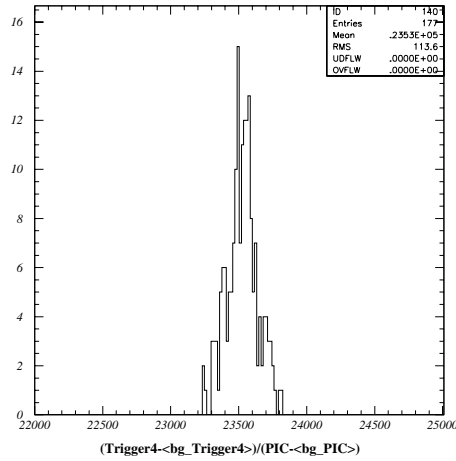


Figure 4: Histogram of $r = \frac{Trigger4 - \langle bg_{Trigger4} \rangle}{PIC - \langle bg_{PIC} \rangle}$ for run number III ($p=120$ GeV/c).

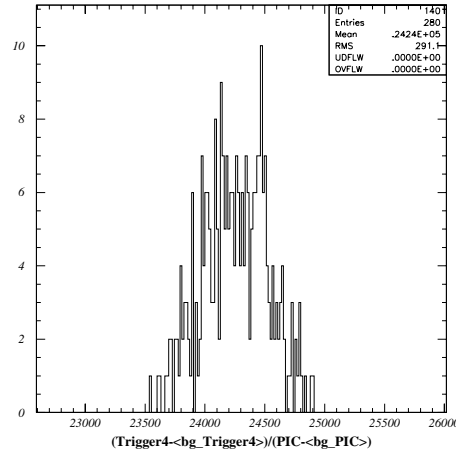


Figure 5: Histogram of $r = \frac{Trigger4 - \langle bg_{Trigger4} \rangle}{PIC - \langle bg_{PIC} \rangle}$ for run number V ($p=40$ GeV/c).

Statistical Error $\Delta\gamma$ of the Calibration Factor γ

For calculating the error $\Delta\gamma$ we can write

$$\langle r \rangle = f(Trigger4, bg_{Trigger4}, \gamma) = \frac{\langle Trigger4_{corr} \rangle}{\langle PIC_{corr} \rangle} = \frac{\langle Trigger4 \rangle - \langle bg_{Trigger4} \rangle}{\frac{1}{\gamma} \langle Trigger4_{corr} \rangle} \quad (2)$$

with γ including all errors of the PIC-counter. Performing an error propagation yields Δr and hence $\Delta\gamma$. Since the value $Trigger4$ is the absolute number of particles crossing the PIC-counter during a spill and since the histogram is filled spill by spill, $Trigger4$ is not subject to any significant error. Therefore we get for Δr

$$(\Delta r)^2 = \left(\frac{\partial f}{\partial bg_{Trigger4}} \right)^2 (\Delta bg_{Trigger4})^2 + \left(\frac{\partial f}{\partial \gamma} \right)^2 (\Delta\gamma)^2. \quad (3)$$

Inserting (2) into Equation (3) yields

$$\Delta r = \sqrt{(\Delta\gamma)^2 + \frac{\langle r \rangle^2}{\langle Trigger4_{corr} \rangle^2} (\Delta bg_{Trigger4})^2}. \quad (4)$$

Solving now for $\Delta\gamma$ gives

$$\Delta\gamma = \sqrt{(\Delta r)^2 - \frac{\langle r \rangle^2}{\langle Trigger4_{corr} \rangle^2} (\Delta bg_{Trigger4})^2} \quad \text{with} \quad \langle r \rangle = \gamma. \quad (5)$$

In order to get the statistical error on the mean value γ we have to divide $\Delta\gamma$ by $\sqrt{entries}$, with $entries$ the number of spills.

Table 6: Calibration values for runs with different intensities at $p=120 \text{ GeV}/c$. Data were taken during 2s counting time.

run number	PIC- bg_{PIC}	calibration factor $\gamma \pm \frac{\Delta\gamma}{\sqrt{entries}}$
I	10.3	24051±81
II	96.4	23481±15
III	117.9	23525±9

Table 7: Calibration values for runs with different intensities at $p=40 \text{ GeV}/c$. Data were taken during 2s counting time.

run number	PIC- bg_{PIC}	calibration factor $\gamma \pm \frac{\Delta\gamma}{\sqrt{entries}}$
IV	11.5	24831±61
V	42.0	24244±17
VI	180.0	24130±7
VII	208.2	24128±6

Tables 6 and 7 show the results. We see that the statistical error is very small. We also find that γ increases significantly for lower intensities.

Systematic Errors of γ

The non linearity of γ as a function of intensity could have several reasons:

- Leaking: if the PIC-counter capacitor leaked during the time between spills, the PIC-counts would be less and the calibration factor would increase.
- Non linearity: a non linearity of the PIC-counter at low intensities could be a possible reason for increasing values of γ .
- Trigger4 dead time correction: if the correction time is set too low, especially the higher Trigger4 values will be affected.

A detailed description of the measurements concerning the first two points can be found in [Gsc00a]. They show that the PIC-counter does not leak and the response of the PIC-counter is linear in a wide range of beam intensities.

The third possible explanation for the non linearity is that the Trigger4 dead time correction of 60 ns is too low. This can be due to the fact that the dead times of the other elements in the read out chain (like the scaler, etc...) are not considered. However, they can also delay the signal and hence calculations of γ for each run I→VII were done with the Trigger4 values dead time corrected with 65 ns and 70 ns, additionally to the ones with 60 ns. Tables 8 and 9 show the results. We see that with a higher dead time τ the discrepancies between low and high intensities decrease.

Table 8: Calibration values calculated with different dead times τ for Trigger4 at $p=120$ GeV/c.

run number	PIC-bg _{PIC}	$\gamma \pm \frac{\Delta\gamma}{\sqrt{\text{entries}}}$		
		$\tau = 60$ ns	$\tau = 65$ ns	$\tau = 70$ ns
I	10.3	24051±81	24071±82	24091±82
II	96.4	23481±15	23631±15	23782±16
III	117.9	23525±9	23711±9	23901±9

Table 9: Calibration values calculated with different dead times τ for Trigger4 at $p=40$ GeV/c.

run number	PIC-bg _{PIC}	$\gamma \pm \frac{\Delta\gamma}{\sqrt{\text{entries}}}$		
		$\tau = 60$ ns	$\tau = 65$ ns	$\tau = 70$ ns
IV	11.5	24831±61	24858±61	24884.7±61
V	42.0	24244±17	24316±17	24388.3±18
VI	180.0	24130±7	24447±7	24775.2±8
VII	208.2	24128±6	24509±6	24897.9±6

PIC calibration factor Γ_{120}^{low} and Γ_{40}

In order to obtain Γ_{120}^{low} and Γ_{40} the factors Γ_{120}^{60ns} , Γ_{120}^{65ns} , Γ_{120}^{70ns} (Γ_{40}^{60ns} , Γ_{40}^{65ns} , Γ_{40}^{70ns}) have to be calculated. We get these factors by taking the weighted average of the three (four) different γ in Table 8 (9) for each Trigger4 dead time correction.

Figure 6 shows the fits for $p=120$ GeV/c. In Figure 7 we see the plots for $p=40$ GeV/c. The results are summarised in Tables 10 and 11.

Table 10: *Fitted PIC calibration factor Γ_{120} of the data at $p=120$ GeV/c for three different Trigger4 dead time corrections.*

$\tau=60$ ns	$\Gamma_{120}^{60ns} = 23519$ particles/PIC-count
$\tau=65$ ns	$\Gamma_{120}^{65ns} = 23695$ particles/PIC-count
$\tau=70$ ns	$\Gamma_{120}^{70ns} = 23875$ particles/PIC-count

Table 11: *Fitted PIC calibration factor Γ_{40} of the data at $p=40$ GeV/c for three different Trigger4 dead time corrections.*

$\tau=60$ ns	$\Gamma_{40}^{60ns} = 24141$ particles/PIC-count
$\tau=65$ ns	$\Gamma_{40}^{65ns} = 24470$ particles/PIC-count
$\tau=70$ ns	$\Gamma_{40}^{70ns} = 24815$ particles/PIC-count

Taking now the mean value of the factors Γ_{120}^{60ns} , Γ_{120}^{65ns} , Γ_{120}^{70ns} and assuming that the difference between the smallest and largest value is $\pm 1\sigma$ allows us to take the systematic effects due to dead time corrections into account. We get for the data taken at 120 GeV/c beam momentum the result

$$\Gamma_{120}^{low} = (23696 \pm 178) \text{ particles/PIC-count.} \quad (6)$$

For the measurements with $p=40$ GeV/c we get

$$\Gamma_{40} = (24475 \pm 337) \text{ particles/PIC-count.} \quad (7)$$

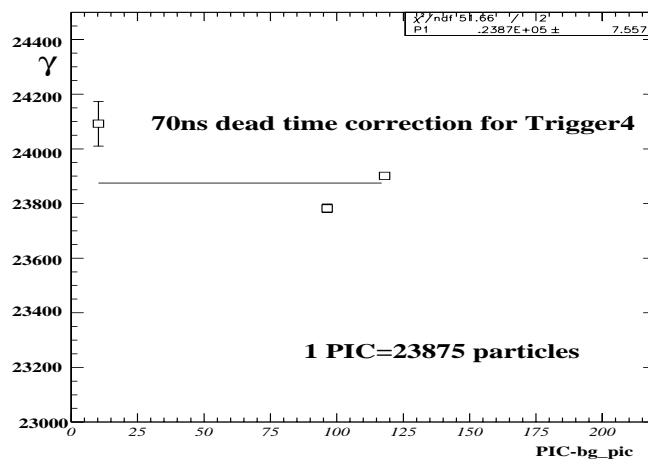
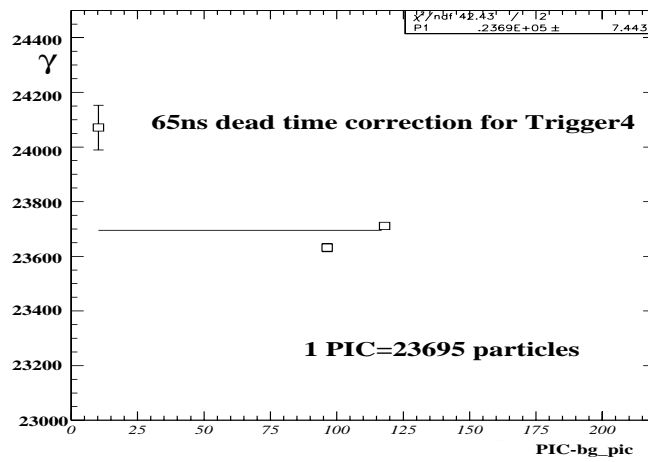
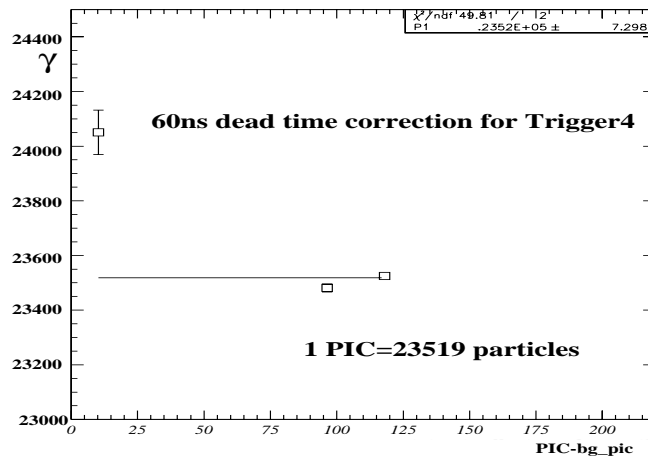


Figure 6: Weighted average of runs with different intensities at $p=120$ GeV/c and different Trigger4 dead time corrections. The statistical errors for the last two values are within the dimensions of the points.

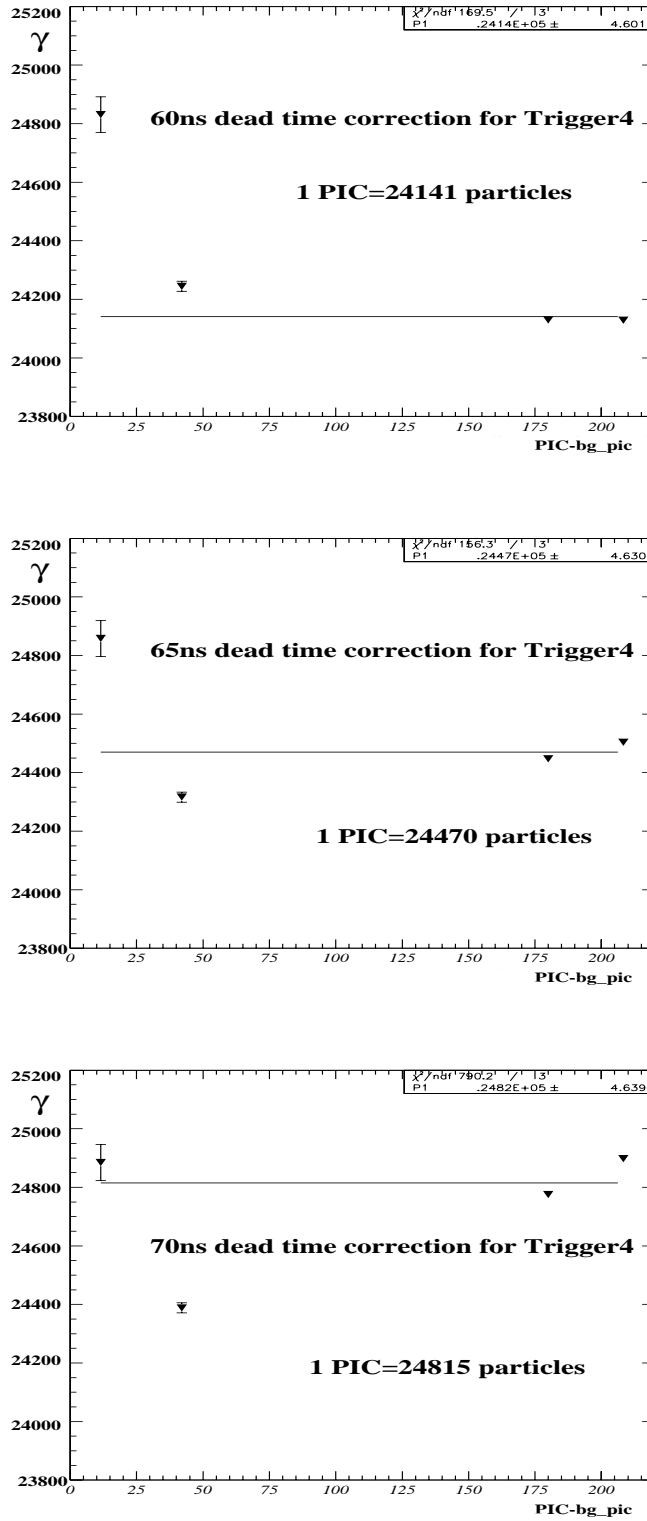


Figure 7: Weighted average of runs with different intensities at $p=40$ GeV/c and different Trigger4 dead time corrections. The statistical errors for the last two values are within the dimensions of the points.

2.4 High Intensity Measurements

The high intensity measurements were performed by varying the beam intensity in the range of 55 to about 8000 PIC-counts per SPS spill. According to the old calibration factor of $2.2 \cdot 10^4$ particles per PIC-count this corresponds to $1.2 \cdot 10^6$ and $1.8 \cdot 10^8$ beam particles per spill, respectively. The beam intensity was changed by adjusting the aperture of collimators C3 and C5. C10 and C11 were kept open at ± 48 mm. Table 12 summarises the raw data obtained for the various collimator settings.

Figure 8 shows the Trigger4 counts per spill as a function of beam intensity, i.e. PIC-counts per spill. At about 700 PIC counts per spill, which corresponds to approximately $1.5 \cdot 10^7$ beam particles per spill, the response of the detector decreases already significantly due to its dead time losses. This is expressed in Figure 8 by the deviation of the points from linearity. Above about 2000 PIC-counts per spill, which gives around $8.8 \cdot 10^7$ beam particles per spill, the response of Trigger4 breaks down completely. In this condition the anode current in the photo-multiplier tube is so high that the potential of the dynodes cannot be kept at their nominal values.

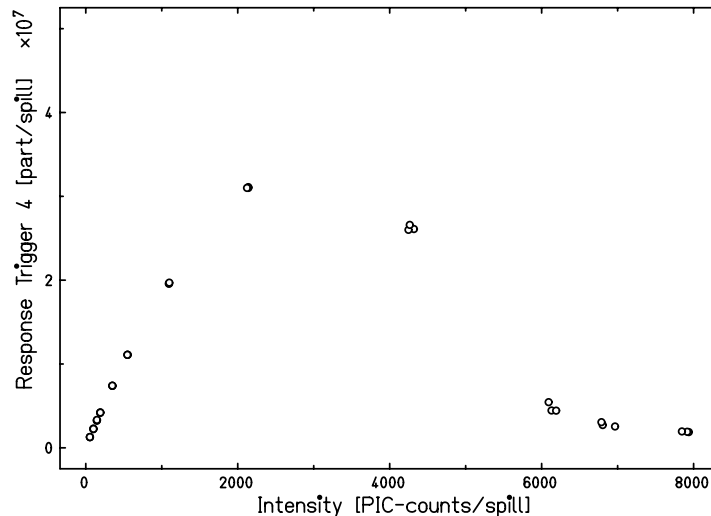


Figure 8: *Trigger4 counts as a function of the beam intensity measured by the PIC. The counting time was the total spill length.*

2.5 Analysis of the High Intensity Measurements

The high beam intensities during the measurements make the correction for dead time losses of Trigger4 the most important task. When calculating the effects of dead time the entire detector system must be taken into account. Usually each element of a detector system has its own dead time, which can be extendable (paralysable dead time model) or non extendable (non paralysable dead time

Table 12: Raw data of the PIC and Trigger4 per SPS spill and per second for different apertures of the collimators C3 and C5.

Collimator Settings		Beam Intensity		Trigger4 Response	
C3	C5	PIC-counts		particles	
[mm]	[mm]	per SPS spill	per second	per SPS spill	per second
±1	±1	55	23.21	$1.28 \cdot 10^6$	$5.40 \cdot 10^5$
		55	23.21	$1.26 \cdot 10^6$	$5.32 \cdot 10^5$
		55	23.21	$1.29 \cdot 10^6$	$5.44 \cdot 10^5$
±2	±1	101	42.62	$2.30 \cdot 10^6$	$9.70 \cdot 10^5$
		99	41.77	$2.23 \cdot 10^6$	$9.41 \cdot 10^5$
		101	42.62	$2.25 \cdot 10^6$	$9.49 \cdot 10^5$
±3	±1	145	61.18	$3.24 \cdot 10^6$	$1.37 \cdot 10^6$
		147	62.03	$3.28 \cdot 10^6$	$1.38 \cdot 10^6$
		148	62.45	$3.32 \cdot 10^6$	$1.40 \cdot 10^6$
±4	±1	190	80.17	$4.17 \cdot 10^6$	$1.76 \cdot 10^6$
		191	80.59	$4.22 \cdot 10^6$	$1.78 \cdot 10^6$
		192	81.01	$4.21 \cdot 10^6$	$1.78 \cdot 10^6$
±4	±2	350	147.7	$7.40 \cdot 10^6$	$3.12 \cdot 10^6$
		351	148.1	$7.39 \cdot 10^6$	$3.12 \cdot 10^6$
		350	147.7	$7.41 \cdot 10^6$	$3.13 \cdot 10^6$
±4	±3	551	232.5	$1.11 \cdot 10^7$	$4.68 \cdot 10^6$
		549	231.6	$1.11 \cdot 10^7$	$4.68 \cdot 10^6$
		548	231.2	$1.11 \cdot 10^7$	$4.68 \cdot 10^6$
±4	±6	1092	460.8	$1.96 \cdot 10^7$	$8.27 \cdot 10^6$
		1096	462.4	$1.96 \cdot 10^7$	$8.27 \cdot 10^6$
		1098	463.3	$1.97 \cdot 10^7$	$8.31 \cdot 10^6$
±4	±12	2140	903.0	$3.11 \cdot 10^7$	$1.31 \cdot 10^7$
		2139	902.5	$3.10 \cdot 10^7$	$1.31 \cdot 10^7$
		2123	895.8	$3.10 \cdot 10^7$	$1.31 \cdot 10^7$
±8	±12	4319	1822	$2.61 \cdot 10^7$	$1.10 \cdot 10^7$
		4248	1792	$2.60 \cdot 10^7$	$1.10 \cdot 10^7$
		4264	1799	$2.66 \cdot 10^7$	$1.12 \cdot 10^7$
±12	±12	6130	2586	$4.46 \cdot 10^6$	$1.88 \cdot 10^6$
		6092	2570	$5.45 \cdot 10^6$	$2.30 \cdot 10^6$
		6192	2613	$4.44 \cdot 10^6$	$1.87 \cdot 10^6$
±12	±14	6965	2939	$2.55 \cdot 10^6$	$1.08 \cdot 10^6$
		6803	2870	$2.71 \cdot 10^6$	$1.14 \cdot 10^6$
		6787	2864	$3.06 \cdot 10^6$	$1.29 \cdot 10^6$
±14	±14	7936	3349	$1.87 \cdot 10^6$	$7.89 \cdot 10^5$
		7915	3340	$1.92 \cdot 10^6$	$8.10 \cdot 10^5$
		7845	3310	$1.96 \cdot 10^6$	$8.27 \cdot 10^5$

model) [Leo87]. The difficulties which often arise are to determine which model is applicable for the entire detector system. Many detector systems are combinations of both, having some elements which are paralyisable and others which are non paralyisable. This makes calculating the effects of dead time very difficult.

Since we did not have any information about the detector components and their dead times our data analysis was done with both models. We assume that they are the two extremes of the experimental set up and our true set up lies in between:

non paralyisable model

$$f' = \frac{f}{1 + \tau f}$$

paralyisable model

$$f' = f \cdot e^{-\tau f}$$

where f' is the measured count rate (in particles per second), f the true count rate (in particles per second) and τ the dead time (in seconds) of Trigger4. Because the PIC does not saturate at these intensities the true count rate of Trigger4 is proportional to the PIC-count rate. The factor of proportionality is exactly the wanted calibration factor Γ of the PIC. This gives us:

non paralyisable model (npm)

paralyisable model (pm)

$$f' = \frac{\Gamma \cdot PICcount\ rate}{1 + \tau \Gamma \cdot PICcount\ rate}$$

$$f' = \Gamma \cdot PICcount\ rate \cdot e^{-\tau \Gamma \cdot PICcount\ rate}$$

From chapter 2.3 we know that the PIC and Trigger4 show a response even if the H6-beam is switched off. Compared to the high PIC-count rate we had, the PIC background is so small that it can be neglected. The Trigger4 background (f'_{bg}) has to be subtracted from the measured Trigger4 count rates:

$$f' - f'_{bg} = \frac{\Gamma \cdot PICcount\ rate}{1 + \tau \Gamma \cdot PICcount\ rate} \Big|_{npm} \quad (8)$$

$$f' - f'_{bg} = \Gamma \cdot PICcount\ rate \cdot e^{-\tau \Gamma \cdot PICcount\ rate} \Big|_{pm} . \quad (9)$$

Shifting f'_{bg} to the right end side

$$f' = \frac{\Gamma \cdot PICcount\ rate}{1 + \tau \Gamma \cdot PICcount\ rate} + f'_{bg} \Big|_{npm} \quad (10)$$

$$f' = \Gamma \cdot PICcount\ rate \cdot e^{-\tau \Gamma \cdot PICcount\ rate} + f'_{bg} \Big|_{pm} \quad (11)$$

we get two equations (10 and 11) which we can use as fit functions through our data points in order to get the PIC calibration factor Γ , the dead time τ and

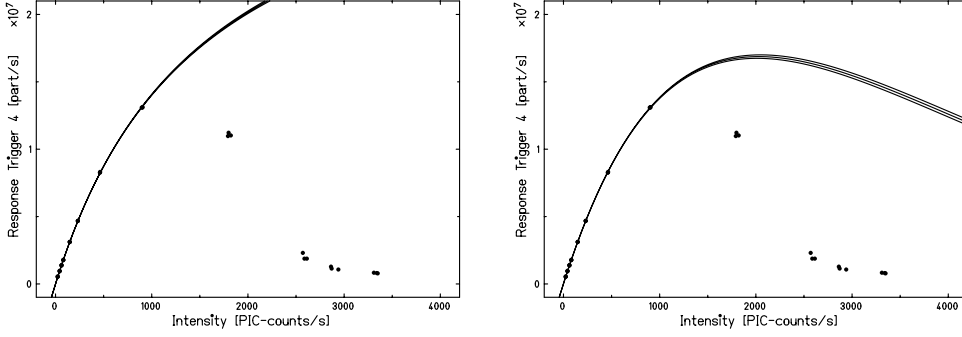


Figure 9: Measured count rate by Trigger4 as a function of the true count rate by the PIC (symbols). **Left:** the solid line is a fit with Equation (10) according to the non paralysable model. **Right:** the solid line is a fit with Equation (11) according to the paralysable model. The experimental data are given per second.

the Trigger4 background f'_{bg} . Figure 9 shows the fit to the data points with the function for the non paralysable model (left) and for the paralysable model (right). The data points above 1700 PIC-counts per second were excluded from the fit because in this region the limit of the photomultiplier electronics is reached and other effects than the Trigger4 dead time are dominating.

For the remaining 24 data points only a rounding error of 0.5% of the Trigger4 values was taken into account. We get this error when recording only two digits after the comma and rounding the third one. The results of the fits are summarised in Table 13.

Table 13: Fit results of the data using Equations (10) and (11) according to the non paralysable model and paralysable model.

Fit parameter	Fit model	
	non paralysable	paralysable
Γ [particles/PIC-count]	23094 ± 68	22567 ± 57
τ [ns]	28.0 ± 0.3	21.8 ± 0.2
f'_{bg} [particles/s]	8437 ± 2491	21096 ± 2299
χ^2/ndf	2.11	1.68

Taking the mean value of the calibration factors obtained from the two different fitting models and assuming that the difference between the smallest and largest value of Γ is the error $\pm 1 \sigma$ we get the final result

$$\Gamma_{120}^{high} = (22831 \pm 264) \text{ particles/PIC-count.} \quad (12)$$

3 Results

PIC calibration factor Γ_{120} at $p=120$ GeV/c

The measurements of Γ give for the low intensity runs (chapter 2.3)

$$\Gamma_{120}^{low} = (23696 \pm 178) \text{ particles/PIC-count.} \quad (13)$$

For the high intensity measurements (chapter 2.4) we get

$$\Gamma_{120}^{high} = (22831 \pm 264) \text{ particles/PIC-count.} \quad (14)$$

We can now calculate the final calibration factor Γ_{120} by taking the mean value of these two totally independent measurements. Its error consists of two contributions, first the error of the two results and second an additional error of 4% which comes from the uncertainty of the HV setting. This gives us the final calibration factor

$$\Gamma_{120} = (23264 \pm 945) \text{ particles/PIC-count.} \quad (15)$$

PIC calibration factor Γ_{40} at $p=40$ GeV/c

In chapter 2.3 we find for the $p=40$ GeV/c measurements

$$\Gamma_{40} = (24475 \pm 337) \text{ particles/PIC-count.} \quad (16)$$

Comparing Γ for $p=40$ GeV/c and $p=120$ GeV/c

Increasing the energy changes the particle composition of the beam and also the energy loss of the single beam particles. Since the PIC-counter is an ionisation chamber we expect a difference of the PIC calibration factor Γ for the two different beam momenta $p=40$ GeV/c and $p=120$ GeV/c. Knowing the beam components and their energy losses for different beam energies we can estimate that the energy loss in the PIC-counter at $p=40$ GeV/c is $\approx 5\%$ lower than at $p=120$ GeV/c. This is consistent with the measurements where Γ_{40} and Γ_{120} differ by $\approx 5\%$.

4 Summary and Conclusion

The PIC-counter was calibrated using the Trigger4 beam scintillator. Two independent measurements with different data processing and analysis methods were performed.

The measurements with low beam intensities were done in the period from 5 to 13 August 1999 within the 'ATLAS Background Benchmarking Measurements'. Three runs were performed with a beam of $p=120$ GeV/c, four runs with $p=40$ GeV/c. The signals of the PIC and the Trigger4 were counted for more than 100 spills. For each run the ratio between the Trigger4 counts and the PIC-counts (both dead time corrected and background subtracted) was histogrammed. This yields a calibration factor γ . A global calibration factor Γ for the $p=120$ GeV/c ($p=40$ GeV/c) runs was then obtained by taking the weighted average of the three (four) factors γ . Systematic errors due to dead time corrections were considered by calculating γ and hence Γ_{120}^{low} (Γ_{40}) for different dead times.

The measurements with high beam intensities were performed in May 1999 during the CERF test-beam period with $p=120$ GeV/c. The intensity ranged from $1.2 \cdot 10^6$ particles per SPS spill to $1.8 \cdot 10^8$ particles per spill. The signal of the PIC was read out online by a LabView program running on a PC. The Trigger4 counts were provided directly by a SPS-beam-control program. The data of three spills per beam intensity were acquired. The calibration factor Γ_{120}^{high} for the PIC resulted from fits through the raw data according to the model for paralyzable and non paralyzable dead time.

The combination of the two experiments gives the final calibration factor Γ_{120} of

$$\Gamma_{120} = (23264 \pm 945) \text{ particles/PIC-count.}$$

Knowing the beam composition in the H6-beam line and the energy loss of the beam particles we can estimate that the beam energy loss in the PIC-counter for $p=40$ GeV/c is about 5% lower than for $p=120$ GeV/c. This is consistent with the low intensity measurements for $p=40$ GeV/c where Γ_{40} is

$$\Gamma_{40} = (24475 \pm 337) \text{ particles/PIC-count.}$$

These results specify the calibration factor of (22000 ± 2200) particles per PIC-count used since 1993.

References

- [Ard00] G. Arduini: private communication, 2000
- [Bir97] C. Birattari, T. Rancati, A. Ferrari, M. Höfert, T. Otto, M. Silari: Recent Results at the CERN-EC High Energy Reference Field Facility. In: *Proc. of the Third Specialists Meeting on Shielding Aspects of Accelerators, Targets and Irradiation Facilities (SATIF-3) at Tohoku University, Sendai, Japan*, ed. by OECD, 1998, pp. 219–234
- [Car93] A. Carlsson, M.C. Hooper, J. Liu, S. Roesler, G.R. Stevenson: SL-RP Measurements during the July 1993 CERN-CEC Experiments. CERN/TIS-RP/TM/**93-32**, 1993
- [Els98] K. Elsener, M. Heilmann, M. Silari: Verification of the calibration factor of the CERF beam monitor. CERN/TIS-RP/TM/**98-22**, 1998
- [Gsc00a] E. Gschwendtner, A. Mitaroff, T. Otto: Performance Tests of the CERF Beam Monitor. CERN/TIS-RP/TM/2000-07, 2000
- [Gsc00b] E. Gschwendtner, C.W. Fabjan, T. Otto, H. Vincke: Measuring the Photon Background in the LHC-Experimental Environment. In: *Proc. of the International Workshop on Neutron Field Spectrometry in Science, Technology and Radiation Protection at Pisa, Italy*, submitted to NIM, 2000
- [Hoo93] M.C. Hooper, C. Raffnsøe, G.R. Stevenson: Beam Monitoring in the May 1993 CERN-CEC Experiment. CERN/TIS-RP/TM/**93-21**, 1993
- [Leo87] William Leo: *Techniques for Nuclear and Particle Physics Experiments*. Springer, 1987
- [Liu93] J. Liu, S. Roesler, G.R. Stevenson: Carbon-11 In Beam Measurements during the September 1993 CERN-CEC Experiments. CERN/TIS-RP/TM/**93-43**, 1993
- [Roe94] S. Roesler, G.R. Stevenson: Carbon-11 measurements during the May 1994 H6 runs. CERN/TIS-RP/TM/**94-10**, 1994
- [Ste94a] G.R. Stevenson, J. Liu, K. O'Brian, J. Williams: Beam Intensity Measurements using ^{11}C Activation for the CERN-CEC Experiments. CERN/TIS-RP/TM/**94-15**, 1994
- [Ste94b] G.R. Stevenson, M.C. Hooper, M. Huhtinen, J. Williams: Measurements of Neutron Yield using a REM-counter and In-Beam C-11 Activation during the H6A94 runs at the CERN-CEC Reference Field Facility. CERN/TIS-RP/TM/**94-26**, 1994
- [Vin99] H. Vincke: private communication, 1999